AD-A114 342 WISCONSIN UNIV-MADISON DEPT OF PHYSICS F/G 7/4
MOLECULAR REACTION RATES.(U)
FEB 82 C C LIN, S CHUNG F19628-79-C-0045
UNCLASSIFIED AFGL-TR-82-0062 NL

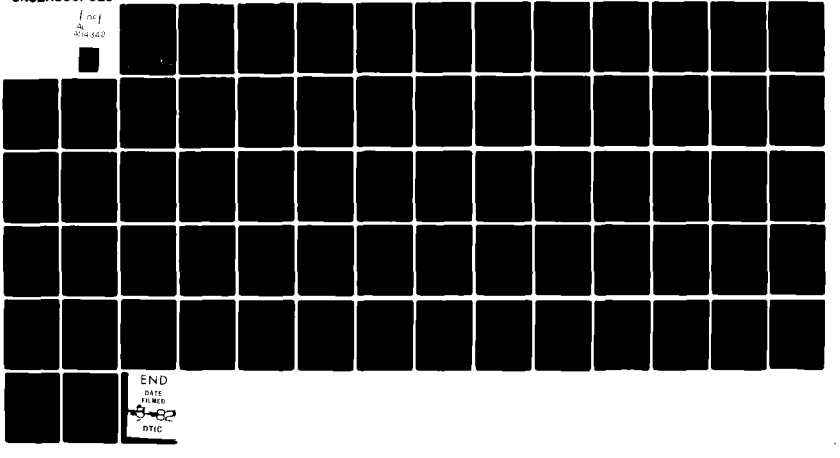

END
DATE FILMED
5-82
DTIC

AFGL-TR-82-0062

MOLECULAR REACTION RATES

Chun C. Lin
Sunggi Chung

Department of Physics
University of Wisconsin-Madison
Madison, Wisconsin 53706

Final Report
15 December 1978 - 26 January 1982

24 February 1982

Approved for public release; distribution unlimited

AIR FORCE GEOPHYSICS LABORATORY
AIR FORCE SYSTEMS COMMAND
UNITED STATES AIR FORCE
HANSCOM AFB, MASSACHUSETTS 01731

Unclassified

SECURITY CLASSIFICATION OF THIS PAGE (When Data Entered)

REPORT DOCUMENTATION PAGE		READ INSTRUCTIONS BEFORE COMPLETING FORM
1. REPORT NUMBER AFGL-TR-82-0062	2. GOVT ACCESSION NO.	3. RECIPIENT'S CATALOG NUMBER
4. TITLE (and Subtitle) Molecular Reaction Rates		5. TYPE OF REPORT & PERIOD COVERED Final 15 Dec. 1978 - 26 Jan. 1982 6. PERFORMING ORG. REPORT NUMBER
7. AUTHOR(s) Chun C. Lin Sunggi Chung		8. CONTRACT OR GRANT NUMBER(s) F19628-79-C-0045
9. PERFORMING ORGANIZATION NAME AND ADDRESS Department of Physics University of Wisconsin-Madison Madison, Wisconsin 53706		10. PROGRAM ELEMENT, PROJECT, TASK AREA & WORK UNIT NUMBERS 61102F 2310G4AH
11. CONTROLLING OFFICE NAME AND ADDRESS Air Force Geophysics Laboratory Hanscom AFB, Massachusetts 01731 Monitor/Edward T. P. Lee/OPR		12. REPORT DATE 24 February 1982 13. NUMBER OF PAGES 70
14. MONITORING AGENCY NAME & ADDRESS(if different from Controlling Office)		15. SECURITY CLASS. (of this report) Unclassified 15a. DECLASSIFICATION/DOWNGRADING SCHEDULE

16. DISTRIBUTION STATEMENT (of this Report)

Approved for public release; distribution unlimited

17. DISTRIBUTION STATEMENT (of the abstract entered in Block 20, if different from Report)

18. SUPPLEMENTARY NOTES

19. KEY WORDS (Continue on reverse side if necessary and identify by block number)

Electron excitation; Electron-molecule collision; Excitation of molecules; Method of close-coupling; R-Matrix method; Polarized-orbital Method; Transition Probability; Lifetime; Multiconfiguration wave function.

20. ABSTRACT (Continue on reverse side if necessary and identify by block number)

Theoretical excitation cross sections of N_2^+ molecule by electron-impact are calculated by the close-coupling method. Excitation cross sections of H_2 are calculated by a hybrid method of close-coupling and the R-Matrix method and by the close-coupling with polarized orbitals included. The transition probability of atomic oxygen $^1S_o \rightarrow {}^1D_2$ (λ = 5577Å) is calculated by using multiconfiguration wave functions.

DD FORM 1 JAN 73 1473 EDITION OF 1 NOV 65 IS OBSOLETE

Unclassified

SECURITY CLASSIFICATION OF THIS PAGE (When Data Entered)

PREFACE

Progress in theoretical research has been continuing toward a better understanding of collision processes of various kinds involving atoms, molecules and electrons. High-speed computers and accumulation reservior of numerical techniques as well as computed and measured data have contributed to creating a progressively favorable condition, from which new ideas are tested, and further progress is made.

In Part I of this report, we have applied the close-coupling method to the electron-N_2 collision problem and calculated excitation cross sections of the Lymann-Birge-Hopfield band. Although the method of close-coupling remains to be a very powerful theoretical tool, its effectiveness can be further increased substantially, if its advantageous features are combined with those of the R-Matrix method. This is described in Part II with the electron-H_2 collision as an example.

In Part III attention is directed to slow-electron collision with molecule, in which the characteristic feature of target polarization is treated by means of the polarized-orbital method. Part IV deals with the transition probability of the dipole-forbidden atomic oxygen transition $^1S_o \rightarrow {}^1D_2$ (5577 Å), which is an important parameter in many applications in the earth's upper atmosphere. The transition probability has been calculated with multiconfiguration Hartree-Fock wave functions.

PART I

ELECTRON-IMPACT EXCITATION CROSS SECTIONS OF THE $a^1\Pi_g$ OF THE N_2 MOLECULE BY THE CLOSE-COUPLING METHOD

I. INTRODUCTION

For a variety of research fields (e.g., geophysics, laser physics), the electron-impact excitation of electronic states of molecules provides basic information.[1-3] Theoretical methods of calculating excitation cross sections for electronic states of diatomic molecules range from the Born approximation,[4,5] the impact-parameter,[6] and distorted-wave[7] methods to the close-coupling method.[8,9] This paper reports excitation cross sections of $N_2(X^1\Sigma_g^+ \rightarrow a^1\Pi_g)$ by a two-state close-coupling (CC) calculation for 12.5 - 50 eV range of incident electron. Within the framework of a two-state close-coupling, the calculations are performed without further approximations. In particular, although there are well-reasoned techniques[9-12] of approximating electron exchange, no recourse is made to them. The cross sections are averaged over the orientation of the molecule with respect to the direction of incident electron. This is equivalent to averaging the cross sections over the initial rotational substates and summing over the final rotational substates, to a very good approximation.[13] The electronic states are assumed to be "vibrationless" with the vertical excitation energy $\Delta E = 9.1$ eV. Thus, the cross sections to a particular vibrational level of the $a^1\Pi_g$ state may be computed by using the Franck-Condon-factor approximation.

The formulation of the close-coupling method[14] is briefly recounted in Sec. II, and the details of calculation is presented in Sec. III. In Sec. IV comparisons are made with the Born-type calculations and with experimental cross sections. A short discussion in Sec. V concludes this paper.

II. CLOSE-COUPLING METHOD

Since a detailed account of the close-coupling method as applied to electronic excitation of molecules is already presented in Ref. 8 (hereafter referred to as CL), only a brief summary is outlined in this section. As in CL the molecule-fixed frame of reference is used here. Then the scattered electron and target, taken together as a collision system, are characterized by the component of the angular momentum along the molecular axis Λ and the spin quantum numbers S,M. The target wave functions are appropriate linear combinations of the Slater determinants consisting of one-electron orbital functions $\phi_j(n_j\lambda_j|\vec{r})$, where λ_j is the projection of angular momentum on the molecular axis and n_j is used to distinguish orbitals of same symmetry λ_j. The scattered-electron function is decomposed into partial waves characterized by angular momenta ℓ and m ($= \Lambda - \lambda_j$). A short notation $\mu = (n\lambda\ell)$ is used to designate a channel.

In the notation of CL the integro-differential equation for the scattered-wave function $F_{\mu'\mu}$ is:

$$\left(\frac{d^2}{dr^2} - \frac{\ell'(\ell'+1)}{r^2} + k'^2\right) F_{\mu'\mu}(r)$$

$$= 2\Sigma_{\mu''} \left[U_{\mu'\mu''}(r) + W_{\mu'\mu''}(r)\right] F_{\mu''\mu}(r)$$

$$+ \Sigma_j \Sigma_\ell \, \delta_{\ell,\ell'} \delta_{\lambda_j,\Lambda-\lambda'} \, M_{n_j\lambda_j\ell} \, \phi_{j,\ell}(n_j\lambda_j|r), \qquad (1)$$

where U and W are respectively the direct and exchange potentials as defined in Eqs. (16) and (17) of CL. The second term on the right-hand side of Eq. (1) is to ensure that $F_{\mu'\mu}$ are orthogonal to the target orbitals by means of the Lagrange multipliers $M_{n_j\lambda_j\ell}$. Here, the two-center molecular orbital functions ϕ_j are expanded about the center of the molecules as

$$\phi_{j,\ell}(n_j\lambda_j|r) = \int d\hat{r}\, Y^{*}_{\ell,\lambda_j}(\hat{r})\, \phi_j(n_j\lambda_j|\vec{r}). \tag{2}$$

The boundary conditions,

$$F_{\mu'\mu}(r) \to 0 \quad \text{as} \quad r \to 0,$$

$$F_{\mu'\mu}(r) \sim (k')^{-\frac{1}{2}} \left[\delta_{\mu'\mu} e^{-i[k'r - \ell'\pi/2]} - e^{i[k'r - \ell'\pi/2]} S^{SM\Lambda}_{\mu'\mu}\right] \quad \text{as } r \to \infty, \tag{3}$$

determine the scattering matrix $S^{SM\Lambda}_{\mu'\mu}$, from which cross sections are obtained (with the initial- and final-state spins $s=s'=0$, and the total spin $S=M=\frac{1}{2}$),

$$Q^{\Lambda}(n\lambda\ell \to n'\lambda'\ell') = (\pi/k^2)\left|1 - S^{\Lambda}_{n'\lambda'\ell',n\lambda\ell}\right|^2, \tag{4}$$

$$Q^{\Lambda}(n\lambda \to n'\lambda') = \Sigma_{\ell\ell'}\, Q^{\Lambda}(n\lambda\ell \to n'\lambda'\ell'). \tag{5}$$

For the discussion that follows, we also define

$$Q(n\lambda\ell \to n'\lambda'\ell') = \Sigma_{\Lambda}\, Q^{\Lambda}(n\lambda\ell \to n'\lambda'\ell'), \tag{6}$$

and

$$Q(n\lambda \to n'\lambda') = \sum_{\Lambda=-\infty}^{+\infty} \sum_{\ell=|\Lambda-\lambda|}^{\infty} \sum_{\ell'=|\Lambda-\lambda'|}^{\infty} Q^{\Lambda}(n\lambda\ell \to n'\lambda'\ell'). \tag{7}$$

In order to facilitate the computation in practical applications, the spherical coordinate system is adopted in the treatment of electronic excitation of molecules, inspite of the fact that diatomic molecules have only an axial symmetry rather than a spherical one. Thus, in this approach, a truncation of partial waves ℓ is inevitable. The summations over ℓ and ℓ' in Eq. (7) underscore this point. This trunication can be recovered with the aid of a partial-wave analysis of the Born approximation. For a given

electronic excitation ($n\lambda \rightarrow n'\lambda'$), the partial cross sections by CC, $Q^{(CC)\Lambda}(\ell,\ell')$ and by Born approximation, $Q^{(B)\Lambda}(\ell,\ell')$ differ substantially for small $(\ell\ell')$, but approach each other for large $(\ell\ell')$. This permits one to compute partial cross sections for $(\ell\ell')$ up to a suitably large L, and use the Born partial cross sections for $(\ell\ell') > L$, with the result

$$Q^{(CC)} \simeq \sum_{\ell\ell'}^{L} \Sigma_\Lambda \, Q^{(CC)\Lambda}(\ell,\ell') + \sum_{\ell\ell'>L} \Sigma_\Lambda Q^{(B)\Lambda}(\ell,\ell')$$

$$= Q^{(BT)} + \sum_{\ell\ell'}^{L} \left(\Sigma_\Lambda [Q^{(CC)\Lambda}(\ell,\ell') - Q^{(B)\Lambda}(\ell,\ell')]\right), \qquad (8)$$

where $Q^{(BT)}$ is the total cross section by the Born approximation. This procedure is found to be quite satisfactory here as it was in other e-molecule collision problems.[8,15]

III. DESCRIPTION OF CALCULATION

A. N_2 wave functions

The ground ($X^1\Sigma_g^+$) and excited ($a^1\Pi_g$) states are derived from the following configurations,[15]

$$X^1\Sigma_g^+: (1\sigma_g)^2(1\sigma_u)^2(2\sigma_g)^2(2\sigma_u)^2(1\pi_u)^4(3\sigma_g)^2,$$

$$a^1\Pi_g: (1\sigma_g)^2(1\sigma_u)^2(2\sigma_g)^2(2\sigma_u)^2(1\pi_u)^4(3\sigma_g)(1\pi_g) .$$

The self-consistent-field (SCF) method[17] is used to calculate the wave functions by applying it to the $X^1\Sigma_g^+$ state and to the $a^1\Pi_g$ state at the equilibrium separation (R_o = 2.0675 a_o) of the ground state. For the basis functions, we have used the set of Gaussian-type orbitals (GTO) consisting of ten 1s-type and six 2p-type GTO's which are contracted to five and four contracted GTO's respectively as given by Dunning.[18] In the notation of Ref. 18, this set reads (10,6)/[5,4]. The total energy of -108.903 76 a.u. is obtained for the $X^1\Sigma_g^+$ state, and -108.434 29 a.u. for the $a^1\Pi_g$ state in the present work. In a comparable calculation by using a similar (9,5)/[5,3] GTO basis set of Dunning,[19] Truhlar et al.[20] obtained the energy ($X^1\Sigma_g^+$) of -108.8890 a.u. They[20] improved the wave function by including two 3d-type GTO's in the basis, i.e., by using (9,5,2)/[4,3,2] set, with the resulting energy of -108.9732, which is compatible with Nesbet's earlier calculation[21] with the Slater-type orbitals (STO) as basis (including 3d-type). The qualities of these and other wave functions are compared in some detail by Eades et al.[22] The present (10,6)/[5,4] wave functions are expected to be of similar quality as the (9,5)/[5,3] functions of Ref. 20. In our previous Born-approximation calculation,[4] the use

of Nesbet's wave functions[21] yielded the $a^1\Pi_g$ cross sections which are about 6% larger than the results obtained by using the GTO functions similar to the ones used in this work.

Strictly speaking, the orbitals in the $X^1\Sigma_g^+$ function do not satisfy the orthonormality relation with those in the $a^1\Pi_g$ function. However, each orbital in one set is very close to the corresponding one in the other; in the worst case, the overlap of $3\sigma_g$ orbitals of the $X^1\Sigma_g^+$ and $a^1\Pi_g$ states is 0.9986. The orthogonality between orbitals belonging to the two states is found to be within 3×10^{-4} except for the overlap 0.0440 between the $2\sigma_g$ and $3\sigma_g$ orbitals. Accepting these small deviations, we used all the orbitals of the $X^1\Sigma_g^+$ state as common to both states except $1\pi_g$ orbital in order to facilitate the computation. The Gaussian exponents and the corresponding coefficients of the orbitals used in this work are shown in Table I.

B. Coupling Potentials

The method of computing the scattering potentials are minutely detailed in CL; in this subsection the particulars pertaining to N_2 ($X^1\Sigma_g^+ \rightarrow a^1\Pi_g$) are discussed. The direct coupling potentials are due to interaction of scattered electron with the nuclei (V^N), and with the bound electrons (V^e), viz.,

$$V^N_{\mu,\mu'}(r) = -\delta_{(n\lambda),\,(n'\lambda')} Z \int d\hat{r}\, Y^*_{\ell,\Lambda-\lambda}(\hat{r}) Y_{\ell',\Lambda-\lambda'}(\hat{r}) \times [|\vec{r}_A - \vec{r}|^{-1} + |\vec{r}_B - \vec{r}|^{-1}], \tag{9}$$

$$V^e_{\mu,\mu'}(r) = \int d\hat{r}\, Y^*_{\ell,\Lambda-\lambda}(\hat{r})\, Y_{\ell',\Lambda-\lambda'}(\hat{r}) \times \Sigma_j f_j \int \phi^*_j(\vec{r}')|\vec{r} - \vec{r}'|^{-1}\phi'_j(\vec{r}')d\vec{r}', \tag{10}$$

where Z (=7) is the nuclear charge, and $\vec{r}_A$, $\vec{r}_B$ are the position vectors of the two nuclei. In Eq. (10) the summation over j indicates the appropriate pairs of molecular orbitals ϕ_j and ϕ_j', and f_j are purely numerical factors. These potentials are computed numerically by the method described in Secs. III and IV of CL. All 14 electrons of N_2 are fully taken into account in this work.

The exchange potentials are integral operators, which may be written as [Eq. (46) of CL]

$$W_{\mu\mu'}(r)F_{\mu'\mu''}(r) = -\Sigma_j g_j \sum_{K,g}\left(\frac{4\pi}{2K+1}\right) r \int d\hat{r} Y^*_{K,g}(\hat{r}) \times Y^*_{\ell,\Lambda-\lambda}(\hat{r})\phi_j'(\vec{r}) \left[\left(r^{-K-1}\int_0^r r'^{K} F_{\mu'\mu''}(r')dr' + r^K \int_r^\infty r'^{-K-1} F_{\mu'\mu''}(r')dr'\right) r' \int d\hat{r}' Y_{K,g}(\hat{r}')Y_{\ell',\Lambda-\lambda'}(\hat{r}') \times \phi_j^*(\vec{r}')\right], \qquad (11)$$

where the summation over j encompasses the appropriate pairs of orbitals ϕ_j and ϕ_j' with numerical factors g_j. Here, the range of K is unbounded. This can be illustrated by considering

$$\sum_K \int d\hat{r}\, Y^*_{K,g}(\hat{r})\, Y^*_{\ell,\Lambda-\lambda}(\hat{r})\phi_j'(\vec{r}) = \sum_{K=|\ell-\ell_j|}^{\ell+\ell_j} \sum_{\ell_j}^{\infty} \int d\hat{r}\, Y^*_{K,g}(\hat{r})\, Y^*_{\ell,\Lambda-\lambda}(\hat{r})\, Y_{\ell_j,\lambda_j}(\hat{r})\phi'_{j,\ell_j}(r), \qquad (12)$$

where the molecular orbital ϕ_j' is decomposed as shown in Eq. (2). Therefore, Eq. (11) can be evaluated only approximately, i.e., with a truncation in the K-series. The results presented in this paper are based on retaining two leading terms of K in Eq. (11). However, we carefully monitored the accuracy of this scheme by repeating the calculation with five such terms included

at a few points with respect to both the incident-electron energy and Λ. The difference in cross sections between the two sets of calculations is quite negligible ($\sim$0.3%), indicating that the two leading terms of K in Eq. (11) were sufficient. As with the direct potential, all 14 electrons are fully taken into account in the exchange potential.

C. Scattering equation

The solution of Eq. (1) by straightforward numerical integration is not possible because of the exchange term which requires a prior knowledge of the solution F(r) for all r as shown in Eq. (11). In the present iterative procedure, (1) the exchange term WF of Eq. (11) is constructed using the F generated in the previous cycle of iteration (we set WF = 0 for the first cycle); (2) using the WF so obtained, new solutions F are calculated; (3) steps (1) and (2) are repeated until a self-consistency is achieved between the successive cycles. This procedure works well for large Λ value and/or at high incident-electron energy, and the cross sections are converged to 0.01% within 4-8 iterations depending on Λ and the incident energy. However, for small Λ or low incident energy, this method fails to give convergent results.[23] In such cases we obtained the solution by the noniterative integral equation method (NIEM) of Smith and Henry.[24] However, NIEM is a much more costly process than an iterative one in terms of computer usage. Therefore, we used the iterative scheme whenever possible (usually for $\Lambda > 3$), and for other cases ($\Lambda = 0 - 3$) we used NIEM. The step-sizes (in units of a_o) used in the numerical integration are $\delta r = 0.0125$ for $0 < r < 1.5$, $\delta r = 0.025$ for $1.5 < r < 3.0$, $\delta r = 0.05$ for $3.0 < r < 5.0$, and $\delta r = 0.1$ for $5.0 < r < 100$. The effective range of exchange potential is about the radial extent of molecular orbitals. In this work the exchange potentials are retained to $r = 8.0\ a_o$, beyond which they are totally negligible. The scattering

matrix $S_{\mu\mu'}$, in Eq. (3) is determined at three different points (r = 50, 75, 100 a_o), and the cross sections are obtained at each point. No significant change in cross sections is found with respect to the "boundary-matching" points.

IV. RESULTS

The excited state $a^1\Pi_g$ is a degenerate state with $\lambda = \pm 1$. We made two separate two-state calculations including one degenerate state each with the ground state. The other option would be to make a three-state calculation. We expect similar results from either set of calculation. In an analogous case of H_2 ($X^1\Sigma_g^+ \rightarrow c^3\Pi_u$) the difference was $\sim$6%.[8]

Since N_2 is a homonuclear molecule, the scattering equations separate into two blocks of even (gerade) and odd (ungerade) symmetry. The partial cross sections, as defined in Eq. (5), at the incident-electron energy E = 50 eV are shown in Table II. For a singlet-singlet excitation the partial cross sections (in series of Λ) converges slowly as seen from Table II. To achieve convergence, the scope of calculation could be expanded, in principle, with respect to ℓ and Λ. An alternative to this procedure is to augment the close-coupling calculation with the Born approximation (BA) as described in Sec. II. The rationale of this procedure is based on the observation that the high ℓ partial waves cannot penetrate close to the target so that the effect of electron-exchange is diminished to the point of insignificance. Under this condition the BA is expected to become valid. This is illustrated in Table III, where comparisons are made of partial cross sections computed by CC and by BA at E = 50 eV. It is seen that the agreement is quite good beyond $\ell > 7$. In other words, the objective of CC is to calculate low ℓ partial cross sections, which the BA overestimates, as shown in Eq. (8). The quantities appearing in Eq. (8) are shown in Table IV at five different energies. The second column shows the total Born cross sections. From the Born total, we replace the Born partial (third column) by the corresponding CC partial (fourth column) to obtain the cross sections (last column). As mentioned before, we included in the calculation interactions between the incident

and all 14 target electrons of N_2 molecule. However, with a view toward future works, we performed test calculations at E = 17 eV, Λ = 1, and even symmetry with (a) $1\sigma_g$ and $1\sigma_u$ omitted, and (b) $1\sigma_g$, $1\sigma_u$, $2\sigma_g$, and $2\sigma_u$ omitted. The resulting cross sections are (a) 0.0472 a_o^2, and (b) 0.0587 a_o^2 as compared with the full calculation value of 0.0487 a_o^2. It is seen that the tightly-bound $1\sigma_g$ and $1\sigma_u$ orbitals could have been excluded from the calculation without significantly ($\sim$3%) changing the final outcome.

The cross sections in Table IV are also plotted in Fig. 1, and compared with the Born-Ochkur results, and experimental measurements.[25,26] The Born-Ochkur approximation (BO) yields good results down to $\sim$30 eV. Since the success of BO is largely phenomenological, it could be used only for a rough estimates of cross sections.

The $X^1\Sigma_g^+ \rightarrow a^1\Pi_g$ excitation has been studied experimentally by numerous groups.[25-32] In Fig. 1 we include two of the latest results by Cartwright et al.[25] and by Finn and Doering.[26] The earlier experiments [27-32] are discussed in some detail in the these papers.[25,26] There are some differences both in magnitude and shape of the excitation function between the two sets of experimental data shown in Fig. 1. Cartwright et al.[25] attribute the difference in magnitude to the cascade contributions which were not considered by Finn and Doering.[26] The other experimental excitation functions (also without cascade correction) lie generally between the two curves shown in Fig. 1.

The present theory agrees reasonably well with experiments above 30 eV, but the disagreement below 30 eV is apparent. Although there are considerable uncertainties in experiments, all experimental excitation functions show the peak occurring somewhere between 15 and 18 eV. Therefore, a good part of the discrepancy between theory and experiment below 30 eV is likely due to the shortcomings of the two-state close-coupling theory.

From the standpoint of the theoretical formalism employed in a calculation, the two-state close-coupling is the most comprehensive one applied to calculate the cross sections of the $a^1\Pi_g$ state to date, and the Born, Born-Ochkur, or distorted-wave method cannot be expected to outperform the close-coupling, since these methods involve further approximation to the two-state close-coupling. Improvement of wave functions is always desirable; it is more difficult to answer to what extent the computed cross sections are affected by the improvement of wave functions. For an estimate, we recall that the inclusion of 3d-type function affected the cross sections by 6% in the Born-Ochkur calculation.[4] The configuration interaction (CI), as a means of accounting for electron correlation, also needs to be considered. However, Billingsley and Krauss[33] report that the value of quadrupole moment of $N_2(X^1\Sigma_g^+)$ changes from -1.29×10^{-26} (single configuration function) to -1.22×10^{-26} esu-cm^2 (18 configuration function), which indicates much less influence of CI in N_2 than in O_2 where the oscillator strength of the Schumann-Runge system is affected by a factor of 3.[34] Therefore, we believe that the improvement in the wave functions (CI included) will not change the computed cross sections by the two-state close-coupling to the extent of bringing theory and experiment to a satisfactory agreement.

V. CONCLUSION

In summary, two-state close-coupling calculations have been performed to obtain the excitation cross sections of $a^1\Pi_g$ state, augmented by the Born partial wave analysis to handle high ℓ partial waves. The present calculations and experiments are in good accord above 30 eV. In the experimental peak region the weight of experimental evidence points to underestimating of cross sections by the two-state close-coupling. In view of the discussion presented in the last paragraph of Sec. IV, the target polarization (i.e., the distortion of N_2 as the incident electron approaches it) emerges as an important factor to be considered toward a better description of the $X^1\Sigma_g^+ \rightarrow a^1\Pi_g$ excitation process.

To incorporate the target polarization, by such methods as that of the polarized orbitals,[35,36] would add another dimension of complexity to the present theoretical treatment of electronic excitation of molecules. However, efforts should be made in this direction, in view of the significant influence of the polarization effects on the electron-atom collisions.[35-37]

References

1. N. F. Lane, Rev. Mod. Phys. 52, 29 (1980).
2. D. C. Cartwright, J. Geophys. Res. 83, 517 (1978).
3. W. A. Fitzsimmons, L. W. Anderson, C. E. Riedhauser, and J. M. Vrtilek, IEEE J. Quantum Electron. QE-12, 624 (1976).
4. S. Chung and C. C. Lin, Phys. Rev. A 6, 988 (1972).
5. S. Chung and C. C. Lin, Phys. Rev. A 9, 1954 (1974).
6. A. U. Hazi, Phys. Rev. A 23, 2232 (1981); A. U. Hazi, T. N. Rescigno, and A. E. Orel, Appl. Phys. Lett. 35, 477 (1979).
7. T. N. Rescigno, C. W. McCurdy, Jr., V. McKoy, and C. F. Bender, Phys. Rev. A 13, 216 (1976); A. W. Fliflet, V. McKoy, and T. N. Rescigno, J. Phys. B. 12, 3281 (1979); A. W. Fliflet, V. McKoy and T. N. Rescigno, Phys. Rev. A 21, 788 (1980).
8. S. Chung and C. C. Lin, Phys. Rev. A 17, 1874 (1978).
9. C. A. Weatherford, Phys. Rev. A 22, 2519 (1980).
10. M. A. Morrison and L. A. Collins, Phys. Rev. A 17, 918 (1978).
11. L. A. Collins and D. W. Norcross, Phys. Rev. A 18, 467 (1978).
12. D. G. Truhlar and N. A. Mullaney, J. Chem. Phys. 68, 1574 (1978).
13. See, for example, J. D. Craggs and H. S. W. Massey, in Handbuch der Physik, edited by S. Flügge (Springer, Berlin, 1956).
14. See, for example, K. Smith, R. J. W. Henry, and P. G. Burke, Phys. Rev. 147, 21 (1966).
15. F. E. Fajen, PhD. Dissertation, (The University of Oklahoma, 1968) (unpublished); W. R. Garrett, Mol. Phys. 24, 465 (1972).
16. A. Loftus and P. H. Krupenie, J. Phys. Chem. Ref. Data 6, 113 (1977).
17. C. C. J. Roothaan, Rev. Mod. Phys. 23, 69 (1951); 32, 179 (1960); E. Clementi and D. R. Davis, J. Comput. Phys. 1, 223 (1966).

18. T. H. Dunning, Jr., J. Chem. Phys. 55, 716 (1971).

19. T. H. Dunning, Jr., J. Chem. Phys. 53, 2823 (1970).

20. D. G. Truhlar, F. A. Van-Catledge, and T. H. Dunning, Jr., J. Chem. Phys. 57, 4788 (1972).

21. R. K. Nesbet, J. Chem. Phys. 40, 3619 (1964).

22. R. A. Eades, D. G. Truhlar, and D. A. Dixon, Phys. Rev. A 20, 867 (1979).

23. Divergence of solution by such an iterative scheme as described in the text is expected to occur under a certain condition for nonlinear integral equation problems, while the Newton-Ralphson method, for example, is quite impractical for the present work. See, for example, B. Noble, in Nonlinear Integral Equations edited by P. M. Anselone (The University of Wisconsin Press, 1964).

24. E. R. Smith and R. J. W. Henry, Phys. Rev. A 7, 1585 (1973).

25. D. C. Cartwright, A. Chutjian, S. Trajmar, and W. Williams, Phys. Rev. A 16, 1013; ibid. 1041 (1977).

26. T. G. Finn and J. P. Doering, J. Chem. Phys. 64, 4490 (1976).

27. W. L. Borst, Phys. Rev. A 5, 648 (1972).

28. R. S. Freund, J. Chem. Phys. 54, 1407 (1971).

29. J. F. M. Aarts and F. J. De Heer, Physica 52, 45 (1971).

30. R. T. Brinkmann and S. Trajmar, Ann. Geophys. 26, 201 (1970).

31. J. M. Ajello, J. Chem. Phys. 53, 1156 (1970).

32. R. F. Holland, J. Chem. Phys. 51, 3940 (1969).

33. F. P. Billingsley II, M. Krauss, J. Chem. Phys. 60, 2767 (1974).

34. S. Chung and C. C. Lin, Phys. Rev. A 21, 1075 (1980); P. S. Julienne, D. Neumann, and M. Krauss, J. Chem. Phys. 64, 2990 (1976).

35. A. Temkin, Phys. Rev. 107, 1004 (1957); A. Temkin and J. C. Lamkin, Phys. Rev. 121, 788 (1961).

36. Vo Ky Lan, J. Phys. B 4, 658 (1971); N. Feautrier, H. Van Regemorter, and Vo Ky Lan, J. Phys. B 4, 670 (1971).

37. P. G. Burke and J. F. B. Mitchell, J. Phys. B 7, 665 (1974); P. G. Burke and J. F. Williams, Phys. Rev. 34, 325 (1977).

Table 1. Gaussian exponents and coefficients of Molecular orbitals[a]

	Exponents	$1\sigma_g$	$2\sigma_g$	$3\sigma_g$	$1\sigma_u$	$2\sigma_u$	$1\pi_u$	$1\pi_g$
				s-type				
1.	13515.3	.267848	-.061832	-.020724	-.268026	-.057581		
2.	1998.9	.510712	-.117896	-.039516	-.511052	-.109792		
3.	439.998	.887235	-.204816	-.068648	-.887826	-.190736		
4.	120.899	1.357210	-.313308	-.105012	-1.358114	-.291771		
5.	38.4711	1.707996	-.394286	-.132154	-1.709134	-.367182		
6.	13.4578	1.499068	-.445468	-.151914	-1.500043	-.417173		
7.	4.99299	.617055	-.288586	-.100557	-.617432	-.272169		
8.	1.56866	.038373	.052194	.026720	-.039060	.043906		
9.	.580017	-.001891	.192906	.043259	.003375	.202914		
10.	.192300	.000242	.021113	.066815	-.001084	.084141		
				p-type				
11.	35.9115	-.012404	-.379650	.772663	.011917	.365687	.719019	.878103
12.	8.48042	-.012338	-.377602	.768495	.011852	.363715	.715140	.873366
13.	2.70563	-.009788	-.299561	.609666	.009403	.288544	.567338	.692862
14.	.992070	-.000013	-.219433	.376496	-.002036	.141049	.320309	.387665
15.	.372670	-.000055	-.020936	.081507	.000040	.033580	.116054	.150332
16.	.134600	-.000001	-.000648	.010651	.000141	.003745	.011082	.044061

[a]All orbitals except $1\pi_g$ are from SCF calculation for $X^1\Sigma_g^+$; $1\pi_g$ from $a^1\Pi_g$ calculation.

Table II. Partial cross sections as defined in Eq. (5) in units of 0.1 a_o^2 at E = 50 eV.

Λ	$a^1\Pi_g^+$ (λ = +1)		$a^1\Pi_g^-$ (λ = -1)	
	even	odd	even	odd
0	0.230831	0.205208		
1	0.146895	0.137790	0.105154	0.154361
2	0.214090	0.100259	0.094702	0.110489
3	0.134843	0.207456	0.067513	0.048896
4	0.130350	0.119458	0.023791	0.035915
5	0.066402	0.077523	0.016711	0.012731
6	0.033294	0.040752	0.004881	0.008817
7	0.013894	0.019317	0.002909	0.002669
8	0.002889			

Table III. Partial cross sections as defined in Eq. (6) in units of 0.1 a_o^2 at E = 50 eV.

Partial wave (incident)	$Q(\ell, \ell' = \ell-2)$		$Q(\ell, \ell' = \ell)$	
	CC	Born	CC	Born
1			0.107902	0.262280
2	0.007377	0.013718	0.105873	0.474302
3	0.043471	0.063359	0.268442	0.467355
4	0.117896	0.231268	0.290970	0.347980
5	0.092329	0.297826	0.199327	0.226233
6	0.220897	0.273740	0.131745	0.139521
7	0.210181	0.220489	0.082937	0.085231
8	0.167138	0.169191	0.052182	0.052686
9	0.127740	0.128287	0.033137	0.033227

Table IV. Total and partial cross sections in units of a_o^2 by Born and CC as indicated in Eq. (8).

Energy (eV)	Born (Total)	Born (Partial)	CC (Partial)	CC (Total)
12.5	2.34106	2.33871	0.522808	0.525158
17	2.12630	2.10064	0.759899	0.785559
20	1.90152	1.84938	0.823102	0.828316
30	1.35222	1.20701	0.709542	0.854752
50	0.841483	0.735434	0.514158	0.620207

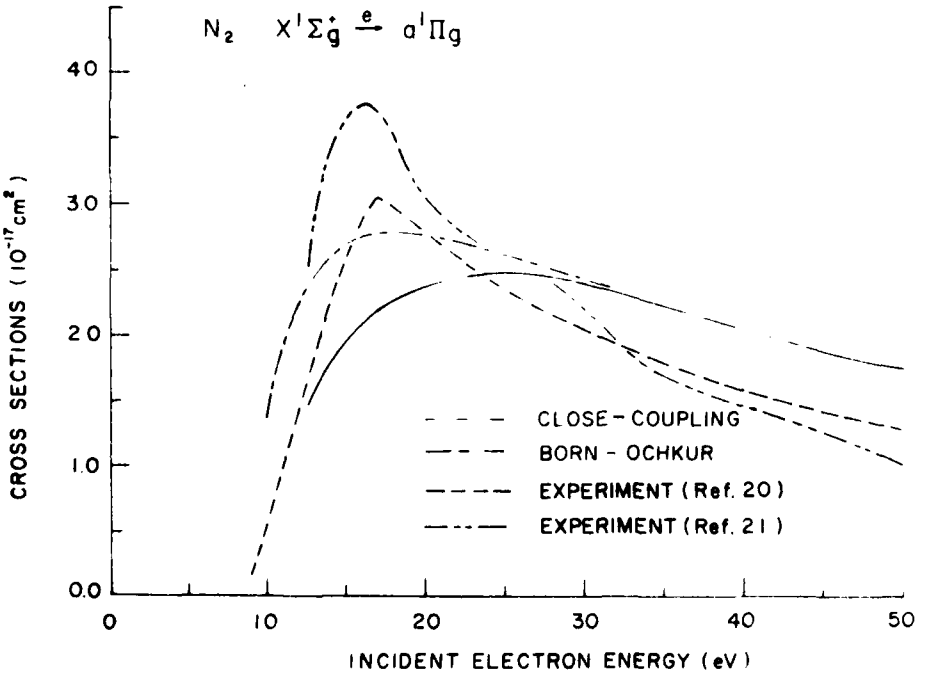

FIG. 1. Excitation cross sections of the $a^1\Pi_g$ state calculated by CC (solid line); by BO (long-short dashed line); and experimental cross sections of Ref. 25 (uniform dashed line); and of Ref. 26 (long-short-short dashed line).

PART II

EXCITATION CROSS SECTIONS OF THE H_2 ($X^1\Sigma_g^+ \rightarrow b^3\Sigma_u^+$) BY THE COMBINED CLOSE-COUPLING-R-MATRIX METHOD

I. INTRODUCTION

For low-energy electron scattering the exchange interaction between the incident electron and the target electrons plays an important role. Particularly in the case of excitation of the target atom (or molecule) with a change in the electron-spin multiplicity, electron exchange is the major interaction responsible for this type of process. While the exchange interaction has been treated in an *ab initio* manner in the theory of electron-atom and electron-molecule excitation based on the method of close coupling (CC),[1-3] the computing cost for this type of calculation is usually quite large. There have been attempts[4] to approximate the electron-exchange; however, the degree of success of these models must be judged ultimately by comparison with the results of the exact treatment of electron-exchange.

The introduction of the R-Matrix (RM) method[5] to atomic physics is largely based on the observation that the effective range of the electron-exchange is confined to the radial extent of the target orbitals (say, $r = a$). The R-Matrix radius a is chosen so that beyond $r = a$ the electron-exchange may be completely ignored. Inside the boundary the electron-exchange is treated rigorously. However, by limiting the radial extent ($r \leq a$), it becomes possible to represent the continuum functions by a finite number of basis functions. Then the scattering equations within the boundary can be solved more efficiently by using the matrix method in contrast to having to solve coupled integro-differential equations in CC. Outside the sphere the exchange terms are neglected so that the CC scattering equations involve no integral operators and can be handled easily.

In the practical application of RM, the choice of basis functions

becomes an important factor with regard to both the efficiency of computation and the accuracy of the results. Various techniques have been used to generate basis functions, including analytic floating Gaussian bases[6] and approximate solutions to the static potential problem without exchange.[5,7] This report describes a practical procedure by which approximate CC solutions are used as a basis for the RM calculation. Such a hybrid CC-RM procedure affords the advantage that a very small basis provides an excellent representation of the scattering solutions within the R-Matrix boundary, and hence greatly reduces the cost of the calculation.

Secs. II and III will outline some key features of CC and RM respectively. No attempt will be made to provide a complete derivation of either procedure, as such derivations can be found in the references cited. Our emphasis will rather be on Sec. IV, in which the scheme for combining the two procedures will be described. In Sec. V a comparison is made of the two sets of excitation cross sections of the $b^3\Sigma_u^+$ state of H_2 computed by the hybrid CC-RM procedure and by the standard CC method.

II. CLOSE-COUPLING METHOD

The details of the close-coupling method as applied to electron-molecule scattering have been presented in Ref. 2, and will not be repeated here. In the molecule-fixed frame of reference, the scattered electron and target, taken together as a collision system, are characterized by the component of the angular momentum along the molecular axis Λ and the spin quantum numbers S,M. The target wave functions are appropriate linear combinations of the Slater determinants consisting of one-electron orbital functions $\phi_j(n_j\lambda_j|\vec{r})$ where λ_j is the projection of angular momentum on the molecular axis and n_j is used to distinguish orbitals of the same symmetry λ_j. The scattered-electron function is decomposed into partial waves of angular momenta ℓ and m $(= \Lambda - \lambda_j)$. The shorthand notation $\mu = (n\lambda\ell)$ will be used to designate a channel. The set of integro-differential equations for the scattered wave functions, $F_{\mu'\mu}$ are

$$\left(\frac{d^2}{dr^2} - \frac{\ell'(\ell'+1)}{r^2} + k'^2\right) F_{\mu'\mu}(r) = 2 \Sigma_{\mu''}[U_{\mu'\mu''}(r) + W_{\mu'\mu''}(r)]F_{\mu''\mu}(r) + (\text{orthogonality}), \tag{1}$$

where U and W are the direct and exchange potentials respectively, and "(orthogonality)" represents the constraints included to ensure that the $F_{\mu'\mu}$ are orthogonal to the target orbitals. The direct coupling potentials are due to the interaction of the scattered electron with the nuclei (U^N), and with the bound electrons (U^e), i.e.,

$$U_{\mu\mu'}(r) = U^N_{\mu\mu'} + U^e_{\mu\mu'}, \tag{2}$$

$$U^N_{\mu\mu'}(r) = -\delta_{(n\lambda),(n'\lambda')}\, Z \int d\hat{r}\, Y^*_{\ell,\Lambda-\lambda}(\hat{r})\, Y_{\ell',\Lambda-\lambda'}(\hat{r}) \times [|\vec{r}_A-\vec{r}|^{-1} + |\vec{r}_B-\vec{r}|^{-1}], \tag{3}$$

$$U^{e}_{\mu\mu'}(r) = \int d\hat{r}\; Y^{*}_{\ell,\Lambda-\lambda}(\hat{r})\; Y_{\ell',\Lambda-\lambda'}(\hat{r})$$

$$\times \Sigma_j f_j \int \phi^{*}_j(\vec{r}')\,|\vec{r}'-\vec{r}|^{-1}\,\phi'_j(r')d\vec{r}', \qquad (4)$$

where Z is the nuclear charge, and $\vec{r}_A$, $\vec{r}_B$ are the position vectors of the two nuclei. In Eq. (4) the summation over j indicates the appropriate pairs of molecular orbitals (MO) ϕ_j and ϕ'_j, and f_j are the corresponding numerical factors (see Ref. 2 for more details). The exchange potentials are integral operators, viz.,

$$W_{\mu\mu'}(r)F_{\mu'\mu''}(r) = -\Sigma_j g_j \Sigma_{K,g} \left[\frac{4\pi}{2K+1}\right] r\int d\hat{r}\; Y^{*}_{K,g}(\hat{r})Y^{*}_{\ell,\Lambda-\lambda}(\hat{r})\phi'_j(\vec{r})$$

$$\times \{[r^{-K-1}\int_0^r r'^{K}F_{\mu'\mu''}(r')dr' - r^{K}\int_0^r r'^{-K-1}F_{\mu'\mu''}(r')dr'$$

$$+ r^{K}\int_0^\infty r'^{-K-1}F_{\mu'\mu''}(r')dr']\; r'\int d\hat{r}'\; Y_{K,g}(\hat{r}')Y_{\ell',\Lambda-\lambda'}(\hat{r}')\phi^{*}_j(\vec{r}')\}, \qquad (5)$$

where, as in Eq. (4), the summation over j covers the appropriate MO's ϕ_j and ϕ'_j with the numerical factors g_j. Because of the third integral in the square bracket, the solution of the integro-differential equations in Eq. (1) takes a great deal of computing time.[2,3] This is a discouraging aspect of CC in practice.

III. R-MATRIX METHOD

Burke and coworkers[5] introduced the R-Matrix method to the electron-atom and electron-molecule scattering problems with detailed derivation of the formulation. It is motivated by the observation that the exchange terms have limited ranges as evidenced by the first integral in Eq. (5). The R-Matrix radius a is chosen such that the exchange is negligible beyond r = a. Thus, outside of this boundary the differential equation of Eq. (1), with WF = 0, can be solved quite expeditiously.

Within the boundary, the scattered waves $F_{\mu',\mu}$ are expanded in terms of chosen basis functions $v_{\mu i}$

$$F_{\mu',\mu}(r) = \Sigma_{i',} c_{\mu' i',\mu} v_{\mu' i'}(r). \tag{6}$$

It is shown in Ref. 5 that diagonalizing the Hamiltonian matrix leads to an equation

$$F_{\mu',\mu}(a) = a \Sigma_{\mu'',} R_{\mu',\mu''} F'_{\mu'',\mu}(a), \tag{7}$$

where F'(a) is the derivative of F(r) at a. The entire interaction of both the direct and exchange types is absorbed in Eq. (7), which relates the scattered-wave functions and their derivatives at r = a. The R matrix is shown to be[5]

$$R = (1/2a)\, \underline{v}^T(a)\, (\underline{H}^S - E\underline{S})^{-1} \underline{v}(a), \tag{8}$$

where H^S is the symmetric part of the Hamiltonian matrix and E is the diagonal energy matrix. The overlap matrix S arises due to the use of nonorthogonal basis functions v.

Eq. (7) is exact and is limited only by the accuracy of the R matrix. The latter in turn depends solely on the basis functions v employed in Eq. (8).

Thus, we see that it is extremely important to devise a means of securing a small but representative basis set in RM. However, this aspect is most wanting in the applications of RM, although several schemes[5-7] have been employed. In the following section, we combine the advantageous features of the RM and CC, thereby gaining a substantial improvement in efficiency over the conventional RM.

IV. HYBRID CC-RM

In the conventional CC approach, the solution of the integro-differential CC equations is quite time-consuming in the vicinity of the molecule where the exchange interaction must be included. This region is exactly the region RM is designed to handle. The most difficult aspect of RM is to generate a small but adequate basis set. On the other hand CC is well suited for providing such a basis set by approximate solution of the CC equations. Thus a combination of the CC and RM may lead to significant improvement over each individual method. Our prescription for a hybrid CC-RM procedure is as follows:

(1) The integro-differential equations [Eq. (1)] of CC are solved iteratively for two iterations as described in IIIC of Ref. 3.

(2) The resulting approximate solutions $\psi_{\mu'\mu}$ ($\psi_{\mu'\mu}$ denotes approximation to $F_{\mu'\mu}$) are used as basis functions v to calculate the R matrix in Eq. (8).

(3) The differential equations for r > a are solved without exchange with Eq. (7) providing the starting solutions.

We describe below each of the steps in some detail.

A. Generation of basis set

In the conventional CC the iterative solutions of Eq. (1) take four or more iterations to converge under favorable conditions.[3] However, in the hybrid CC-RM approach we seek only approximate solutions of Eq. (1) and use them as basis functions, thus two iterations are found to be adequate. Further, these solutions are obtained with the orthogonality constraints with respect to the bound MO's so that the computation of the R matrix in Eq. (8) is simplified. The basis set for a particular exit channel μ' is formed from $\psi_{\mu'\mu}$ with $\mu = 1,2,\ldots,n$ corresponding to all incident channels. These functions $\psi_{\mu'\mu}$ are normalized within the R-matrix boundary (0,a) and redundant ones are

discarded by an overlap criterion. However, the dominant diagonal ones $\psi_{\mu\mu}$ are always retained.

B. Solutions in the exterior region

The RM procedure has served its purpose when R(a) has been obtained. The CC equations without exchange are to be solved in the exterior region from r = a. That is, for r > a Eq. (1) is reduced to

$$\left(\frac{d^2}{dr^2} - \frac{\ell'(\ell'+1)}{r^2} + k'^2\right) F_{\mu'\mu}(r) = 2 \Sigma_{\mu''} U_{\mu'\mu''} F_{\mu''\mu}(r). \tag{9}$$

The orthogonality constraints, like the exchange terms, can be ignored here. The Numerov[8] method is used to generate the solutions until the asymptotic form has been reached, i.e.,

$$F_{\mu'\mu}(r) \sim (1/k'^{\frac{1}{2}})[\delta_{\mu'\mu} e^{-i(k'r-\ell'\pi/2)} - e^{i(k'r-\ell'\pi/2)} S^{SM\Lambda}_{\mu'\mu}]. \tag{10}$$

The cross sections are extracted from the scattering matrix $S^{SM\Lambda}_{\mu'\mu}$ in the usual manner[2],

$$Q^{SM\Lambda}(n\lambda s\ell \to n'\lambda' s'\ell') = (\pi/k^2)|\delta_{\mu'\mu} - S^{SM\Lambda}_{\mu'\mu}|^2, \tag{11}$$

$$Q(n\lambda s \to n'\lambda' s') = \Sigma_S \frac{(2S+1)}{2(2s+1)} \sum_{\Lambda\ell\ell'} Q^{SM\Lambda}(n\lambda s\ell \to n'\lambda' s'\ell'). \tag{12}$$

For the purpose of discussion we also define

$$Q^{SM\Lambda}(n\lambda s \to n'\lambda' s') = \sum_{\ell\ell'} Q^{SM\Lambda}(n\lambda s\ell \to n'\lambda' s'\ell'). \tag{13}$$

The manner in which R(a) is used to construct the starting solutions is now discussed. Near the boundary r = a the true solutions $F_{\mu'\mu}$ can be written as

$$F_{\mu'\mu}(r) = N[J_{\mu'\mu}(r) + Y_{\mu'\mu'}(r) K_{\mu'\mu}(r)], \tag{14}$$

with

$$J_{\mu'\mu}(r) = \delta_{\mu'\mu} k_\mu^{\frac{1}{2}}, r\, j_{\ell_{\mu'}}(k_{\mu'} r), \tag{15}$$

$$Y_{\mu',\mu}(r) = \delta_{\mu',\mu} k_{\mu}^{\frac{1}{2}} r\, y_{\ell_{\mu}}(k_{\mu} r), \tag{16}$$

where j_ℓ and y_ℓ are the spherical Bessel functions of the first and second kinds respectively. Although the K(r≈a) matrix differs from its asymptotic value K(r→∞), we expect that it varies slowly with r in this region so that

$$K(a+\delta r) \approx K(a), \tag{17}$$

the step-size δr being of the order of $0.1\, a_0$. The normalization constant N in Eq. (14) is immaterial and set to 1. By substituting Eq. (14) into Eq. (7), we obtain

$$K(a) = -\,(Y - aRY')^{-1}\,(J - aRJ'), \tag{18}$$

where all matrices are evaluated at r ≈ a, and the prime indicates the derivative with respect to r. Here, we have ignored K'(a) in view of Eq. (17). Thus, with the K matrix as given by Eq. (18), we construct $F_{\mu',\mu}$ at two starting points, viz.,

$$F_{\mu',\mu}(a) = J_{\mu',\mu}(a) + Y_{\mu',\mu'}(a) K_{\mu',\mu}(a), \tag{19}$$

and

$$F_{\mu',\mu}(a+\delta r) = J_{\mu',\mu}(a+\delta r) + Y_{\mu',\mu'}(a+\delta r) K_{\mu',\mu}(a). \tag{20}$$

With these two starting points, the three-point recursion formula of Numerov may be used to perpetuate the solutions to any desired r.

V. RESULTS

The hybrid CC-RM procedure has been used to calculate the excitation ($X^1\Sigma_g^+ \rightarrow b^3\Sigma_u^+$) cross sections of H_2 at incident electron energies of 13, 15, 20, and 30 eV. Since these cross sections have been already calculated by the close-coupling method,[2] a good test of the present procedure can be made by comparison. The wave functions and various potentials employed in this work are identical to those used in the CC calculation.[2] At each incident energy the approximate CC parent basis functions are generated in a numerical tabular form for channel angular momentum up to $\ell = 5$. Redundancy within this parent basis set is removed using a normalized overlap tolerance of 0.9. The resulting basis set is very small, with only two or three basis functions for each exit channel generally. Table I shows a typical number of basis functions used for the calculation of $\Lambda = 0$ and E = 15 eV. The R matrix is then calculated with the boundary $a = 20\ a_0$.

Table II shows the convergence of the partial-wave expansions for a typical (Λ,E) block as defined in Eq. (11) with $S = M = \frac{1}{2}$. The partial cross sections due to the largest ℓ retained are seen to be four to five orders of magnitude smaller than the largest partial cross sections in the block. Since fewer partial waves participate at lower energies, this convergence at E = 30 eV as shown in Table II should guarantee convergence at all lower energies. The convergence with respect to the Λ-expansion is shown in Table III for the incident energy E = 15 eV (near peak). For the excitation of homonuclear molecules, the partial cross sections as well as the differential equations separate according to even and odd parity. The partial cross sections of $\Lambda = 0,1,2$ are shown to be quite sufficient. The agreement between the present hybrid CC-RM and the standard CC results,[2] shown in Table IV and Figure 1, is within 5% at worst. This excellent agreement demonstrates the adequancy

of the small CC basis set. Test calculations with the spherical Bessel functions as basis show that it takes 90 Bessel functions to achieve a similar degree of agreement with the previous close-coupling calculation[2] as the present calculation. The difficulty of achieving convergence with the Bessel functions stems from the fact that the Bessel functions are in reality components of a plane wave, whereas the true scattered functions are considerably phase-shifted and otherwise modified from the plane wave in the interior region.

In general the R matrix boundary a is chosen by compromising the two conflicting requirements: (1) the larger the a, the less of the exchange is ignored; (2) the smaller the a, the better the expansion Eq. (6) becomes with a given number of basis functions. The rather large value of $a = 20\ a_0$ is chosen to provide a very stringent test of the ability of the CC basis to adequately represent the scattering functions in the interior region. The previous CC calculation, to which we compare present results, also included the exchange up to $r = 20\ a_0$. However, the boundary a can be significantly reduced. For example, even for the diffuse $1\sigma_u$ orbital, integration beyond $r = 14\ a_0$ does not contribute more than 10^{-6} to the normalization value of unity. Had we chosen this ($14\ a_0$) or yet smaller value for a, the representation by our present basis functions would have been even better. This would also have reduced the computing cost still more.

V. CONCLUSION

We find that the hybrid CC-RM described in this paper is a far more efficient method than either CC or RM method used separately. From the point of view of CC this method eliminates the time-consuming process of solving the integro-differential equations in the interior region by "borrowing" the matrix method of RM. In the present calculation of H_2 with six channels or less, the overall computer usage was reduced by a factor of about five compared with our earlier work by CC alone. This savings in computing time will increase progressively with number of channels included in the coupled equations. Viewed from the point of RM, it is impressive to see that the scattering functions can be represented by as few as two or three basis functions per channel. We believe this hybrid method will make a very useful tool in dealing with electron scattering from such moderate-size molecules as N_2 or O_2.

REFERENCES

1. See, for example, I. C. Percival and M. J. Seaton, Proc. Camb. Phil. Soc. 53, 654 (1957); K. Smith, R. J. W. Henry, and P. G. Burke, Phys. Rev. 147, 21 (1966).
2. S. Chung and C. C. Lin, Phys. Rev. A 17, 1874 (1978).
3. T. K. Holley, S. Chung, C. C. Lin, and E. T. P. Lee, Phys. Rev. A 24, 2946 (1981).
4. C. A. Weatherford, Phys. Rev. A 22, 2519 (1980); and references therein.
5. P. G. Burke, A. Hibbert, and W. D. Robb, J. Phys. B 4, 153 (1971); P. G. Burke, I. Mackey and I. Shimamura, J. Phys. B 10, 2497 (1977); I. Shimamura, J. Phys. B 13, 2597 (1977).
6. B. I. Schneider, Chem. Phys. Lett. 31, 237 (1975); B. I. Schneider, Phys. Rev. A 11, 1957 (1975); B. I. Schneider, P. J. Hays, Phys. Rev. A 13, 2049 (1976).
7. K. A. Berrington, P. G. Burke, M. Le Dourneuf, W. D. Robb, K. T. Taylor, and Vo Ky Lan, Comput. Phys. Commun. 8, 149 (1974); 14, 367 (1978).
8. See, for example, D. R. Hartree, The Calculation of Atomic Structures (Wiley, New York, 1957), p. 71.

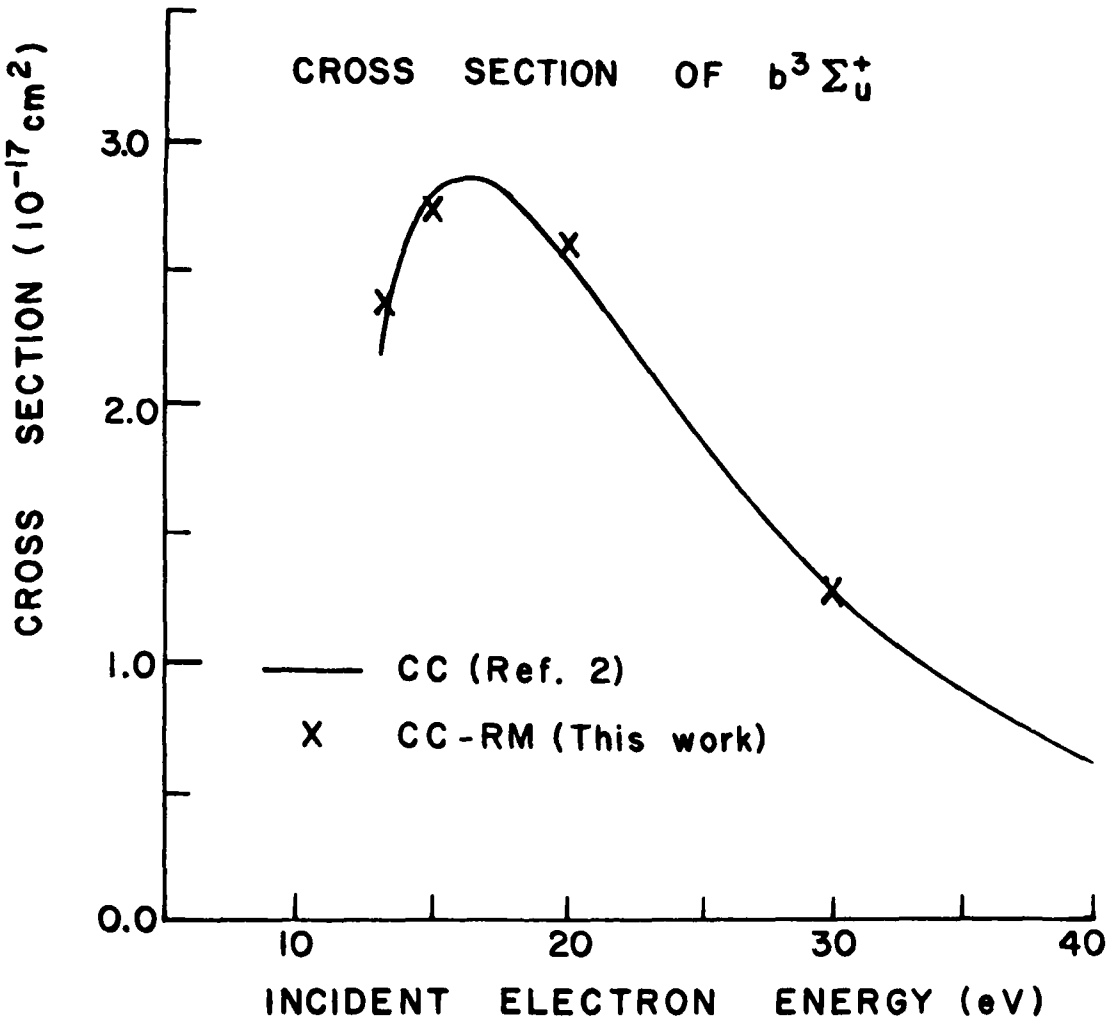

FIG. 1. Excitation cross sections of the H_2 ($X^1\Sigma_g^+ \rightarrow b^3\Sigma_u^+$) by the present hybrid CC-RM method (X); and by the close-coupling method (solid curve).

Table I. The number of basis functions per channel used in Eq.(6) to calculate the Λ=0 (odd) partial cross section at E=15 eV.

Channel	ℓ	Number of basis functions
$X^1\Sigma_g^+$	1	2
	3	3
	5	2
$b^3\Sigma_u^+$	0	4
	2	3
	4	1

Table II. Partial cross sections[a] $Q_{\ell\ell'}^{\Lambda=0}$ as defined by Eq. (11) at E = 30 eV in units of a_o^2.

ℓ/ℓ'	0	1	2	3	4	5
0		0.316 643 (-2)		0.141 749 (-4)		0.168 235 (-5)
1	0.148 627 (0)		0.125 126 (-1)		0.698 513 (-4)	
2		0.460 716 (-4)		0.520 876 (-6)		0.216 455 (-5)
3	0.169 621 (-2)		0.984 064 (-3)		0.858 177 (-4)	
4		0.110 671 (-4)		0.183 979 (-4)		0.939 092 (-5)
5	0.790 265 (-4)		0.108 219 (-4)		0.886 633 (-4)	

[a]Numbers in parentheses denote the power of 10.

Table III. Partial cross sections Q^{Λ} as defined by Eq. (13) at E = 15 eV in units of a_o^2.

Λ	Even Parity	Odd Parity
0	0.010 460	0.434 656
1	0.252 884	0.006 747
2	0.000 159	0.002 684

Table IV. Total excitation cross sections of the $b^3\Sigma_u^+$ state in units of 10^{-17} cm^2.

Energy (eV)	Q (CC-RM)	Q (CC)
13	2.31	2.19
15	2.72	2.80
20	2.63	2.53
30	1.25	1.26

PART III

EFFECT OF TARGET POLARIZATION IN SLOW-ELECTRON COLLISIONS: EXCITATION CROSS SECTIONS OF H_2 ($X^1\Sigma_g^+ \rightarrow B^1\Sigma_u^+$) BY THE POLARIZED-ORBITAL METHOD

I. INTRODUCTION

In the electron-impact processes of atoms and molecules, if the energy of the incident electron is low enough, then the bound electrons of the target atom (or molecule) adjust themselves adiabatically in response to the incoming electron. The distorted atoms in turn interact back with induced multipole moments in form of long-range potentials.[1-4] This is the characteristic feature of slow-electron scattering in contrast to collision by fast electrons. Thus, simple theoretical prescriptions such as the Born approximation are no longer valid. In principle the distortion of the target may be taken into account by including a sufficient number of terms in the close-coupling expansion. Such an expansion may be further improved by including pseudostates in the expansion. This method has shown to be satisfactory in calculating excitation cross sections of atomic H.[5] Alternatively, one may direct attention to the long-range potentials, and construct empirically these potentials from the known static properties of the target atoms. The latter, called pseudopotential method, has been applied to elastic scattering problems on H_2[6] and N_2.[7]

Another approach is the method of polarized orbitals,[3,4] in which adiabatic first-order corrections to the target molecular orbitals are explicitly included as part of the target wave function. The polarized orbitals (correction terms) are calculated with only the dipole component of multipole moments included as the perturbation. With the molecular orbitals (MO) thus expressed as linear superposition of the unperturbed and polarized orbitals, the standard close-coupling (CC) calculation[8] can be carried out to obtain cross sections.

In this report we calculate the excitation cross sections of H_2 ($X^1\Sigma_g^+ \rightarrow B^1\Sigma_u^+$) by a two-state close-coupling with the polarized orbitals

included. A comparison is made with the previous two-state close-coupling calculation without polarized orbitals[8] to assess the influence of the long-range induced potentials.

Sec. II contains a brief description of the polarized-orbital method and numerical procedure for obtaining the polarized orbitals. In Sec. III we describe how these polarized orbitals are utilized to augment the close-coupling equations as well as a brief recount of the close-coupling method. The results and their comparison with the previous calculation with no polarization are presented in Sec. IV.

II. POLARIZED ORBITAL

The purpose of polarized orbitals is to incorporate the characteristic feature of slow-electron scattering into a mathematical formulation, namely, the distortion of target caused by slow electron located at a substantially far distance compared with molecular dimension. In this report we consider only the distortion of the target molecule by the Coulomb interaction of the incident electron. Moreover, since the dipole interaction dominates over other higher multipole terms, we will keep the dipole term only. It will be seen below that this approximation will also facilitate the solutions for differential equations for the polarized orbitals.

Since the theoretical derivations leading to the differential equations for the polarized orbitals are identical in all essential detail to those given by Temkin and co-workers,[3] a brief outline is given below as they relate to the present problem. Next, a numerical procedure[9] of solving inhomogeneous differential equation is described.

A. Formulation

The Hamiltonian for the system consisting of the target H_2 molecule and the scattering electron located at $\vec{r}_3$ is

$$H_{ad} = H_{mol} + H', \tag{1}$$

$$H' = -Z(|\vec{r}_3-\vec{r}_A|^{-1} + |\vec{r}_3-\vec{r}_B|^{-1}) + \sum_{i=1}^{2} |\vec{r}_3-\vec{r}_i|^{-1}, \tag{2}$$

where $\vec{r}_A$, $\vec{r}_B$ are the position vectors of the two nuclei, and Z (=1) is the nuclear charge. We construct a variational trial wave function for the H_2 ground state as

$$\Phi^X = A\,[(1\sigma_g(\vec{r}_1) + 1\sigma_g'(\vec{r}_1|\vec{r}_3))\alpha\ (1\sigma_g(\vec{r}_2) + 1\sigma_g'(\vec{r}_2|\vec{r}_3)\beta], \tag{3}$$

where $1\sigma_g'(\vec{r}_1|\vec{r}_3)$ is the first-order correction to the unperturbed MO $1\sigma_g(\vec{r}_1)$ due to the scattering electron located at $\vec{r}_3$. If the energy of the system is minimized with respect to variations in $1\sigma_g'$, the first-order term yields an equation for the polarized orbital $1\sigma_g'$,

$$(h + V - \varepsilon^o)\ 1\sigma_g' = -H'1\sigma_g, \tag{4}$$

with

$$h = -(1/2)\nabla^2 - Z(|\vec{r}-\vec{r}_A|^{-1} + |\vec{r}-\vec{r}_B|^{-1}), \tag{5}$$

$$V = \int 1\sigma_g^*(\vec{r}_1)|\vec{r}_1-\vec{r}_3|^{-1}1\sigma_g(\vec{r}_1)d\vec{r}_1, \tag{6}$$

and ε^o is the orbital energy of the unperturbed $1\sigma_g$. We now truncate the multipole expansion in Eq. (2), retaining the dipole term only,

$$H' \simeq (4\pi/3)\ \sum_i r_i\ r_3^{-2}\ \Sigma_q\ Y_{1q}^*(\hat{r}_i)Y_{1q}(\hat{r}_3), \tag{7}$$

where $Y_{\ell m}$ is the spherical harmonic. This allows us to write the polarized orbital $1\sigma_g'(\vec{r}_1|\vec{r}_3)$ as a product of functions of $\vec{r}_1$ and of $\vec{r}_3$, viz.,

$$1\sigma_g'(\vec{r}_1|\vec{r}_3) = \sum_{\ell m} r_1^{-1}\phi_{\ell m}(r_1)Y_{\ell,m}(\hat{r}_1)r_3^{-2}Y_{1,-m}(\hat{r}_3). \tag{8}$$

Substitution of Eqs. (7) and (8) into Eq. (4) yields a set of coupled differential equations in $\phi_{\ell m}$ for each m.

$$\left(\frac{d^2}{dr^2} - \frac{\ell(\ell+1)}{r^2} + k^2\right)\phi_{\ell m}(r) = \Sigma_{\ell'}\ U_{\ell\ell'}(r)\phi_{\ell'm}(r) + G_{\ell m}(r), \tag{9}$$

with

$$U_{\ell\ell'}(r) = -2Z\int d\hat{r}\ Y_{\ell m}^*(\hat{r})(|\vec{r}-\vec{r}_A|^{-1} + |\vec{r}-\vec{r}_B|^{-1})Y_{\ell'm}(\hat{r})$$

$$+ 2\int d\vec{r}'d\hat{r}\ 1\sigma_g^*(\vec{r}')Y_{\ell m}^*(\hat{r})|\vec{r}-\vec{r}'|^{-1}1\sigma_g(\vec{r}')Y_{\ell'm}(r), \tag{10}$$

$$G_{\ell m}(r) = -(8\pi/3)r \int d\vec{r}' 1\sigma_g^*(\vec{r}')Y_{1,-m}(\hat{r}')Y_{\ell m}(\hat{r}'), \tag{11}$$

and

$$k^2 = 2|\varepsilon^o|. \tag{12}$$

The differential equations in Eq. (9) resemble close-coupling equations except for the inhomogeneity $G_{\ell m}(r)$, which represent the dipole component of the perturbation caused by the incident electron. The numerical procedure used for the solutions of these equations is described in the next subsection.

B. Numerical Solution

Let us define

$$W_{\ell\ell'} = U_{\ell\ell'} + [\frac{\ell(\ell+1)}{r^2} - k^2]\delta_{\ell\ell'}, \tag{13}$$

and rewrite Eq. (9) in a matrix form

$$\frac{d^2}{dr^2}\underline{\phi} = \underline{W\phi} + \underline{G}, \tag{14}$$

where $\underline{\phi}$ and $\underline{G}$ are viewed as column vectors and $\underline{W}$ a matrix. The physically acceptable solutions $\underline{\phi}$ must satisfy the boundary conditions

$$\phi_\ell(0) = 0, \tag{15}$$

$$\phi_\ell(r) \sim e^{-kr} \text{ as } r\to\infty. \tag{16}$$

The numerical method employed in solving Eq. (14) is similar to the one used by Vo Ky Lan,[9] and consists of replacing the differential equations by the difference equations, i.e.,

$$\sum_{i=-1}^{n-2} a_i^n \underline{\phi}_{i+k} = \underline{W}_k\underline{\phi}_k + \underline{G}_k , \tag{17}$$

where $\underline{\phi}_k$ denotes $\underline{\phi}(r_k)$ etc., and a_i^n is the Lagrange n-point differentiation coefficient at the point r_i. Next, we assume

$$\underline{\phi}_k = \sum_{i=1}^{n-2} \underline{Q}_k^i \underline{\phi}_{k+i} + \underline{C}_k \ . \tag{18}$$

Elimination of $\underline{\phi}_k$ between Eqs. (17) and (18) leads to the identifications,

$$\underline{A}_k = \underline{W}_k - a_0^n - a_{-1}^n \underline{Q}_{k-1}^1, \tag{19}$$

$$\underline{Q}_k^i = (\underline{A}_k)^{-1}[a_i^n + a_{-1}^n \underline{Q}_{k-1}^{i+1}], \ i = 1,2,\ldots,n-2, \tag{20}$$

$$\underline{C}_k = (\underline{A}_k)^{-1}[a_{-1}^n \underline{C}_{k-1} - \underline{G}_k] \ . \tag{21}$$

The boundary conditions of Eqs. (15) and (16) translate to

$$\underline{Q}_0^i = 0, \ \underline{C}_0 = 0. \tag{22}$$

Starting from k = 0, the recursion relations of Eqs. (20) and (21) are used to generate arrays $\underline{Q}_k^i$ and $\underline{C}_k$ to a suitably large $r_{k=Last}$. Then we set $\underline{\phi}_{Last} = 0$, and the inward recursion formula of Eq. (18) is used to generate all $\underline{\phi}_k$.

In our work we adopted five-point Lagrange formula (n=5) in Eq. (17) as opposed to the three-point formula used by Vo Ky Lan.[9] But there is no significant difference between the two schemes. The outward recursion was carried out to 23 - 33 a_o. Satisfactory results are obtained with r_k in this range.

III. SCATTERING EQUATIONS

The scattering equations for a close coupling is well known in the case where unperturbed MO are used only, i.e.,

$$[\frac{d^2}{dr^2} - \frac{\ell(\ell+1)}{r^2} + k_\mu^2] F_{\mu\mu'}(r) = \Sigma_{\mu''}(U_{\mu\mu''} + W_{\mu\mu''}) F_{\mu''\mu'}(r), \tag{23}$$

where $U_{\mu\mu''}$ and $W_{\mu\mu''}$ are direct and exchange potentials respectively. If the polarized orbitals are included in the target state in the manner of Eq. (3), then additional polarization potentials enter Eq. (23) in an analogous way as $U_{\mu\mu''}$ and $W_{\mu\mu''}$.

However, before plunging into calculation, it is worthwhile to review what we are attempting to accomplish with the polarized orbitals in the context of physical situation. Polarized orbitals are to describe the distortion of target molecule when the incident electron is at a distance substantially greater than the molecular dimension. When the incident electron comes within the molecule, all electrons including the incident electron must be treated on an equal-footing. This physical situation cannot be described by polarized orbitals. Therefore, it has been tacitly assumed that the the incident electron always stays outside the molecular electrons. We now make this assumption explicit as suggested in Temkin's original paper.[3] For example, in the expression of the direct potential due to the polarized orbital,

$$\begin{aligned} U^{Pol}_{\mu\mu'}(r) = 2 \Sigma_{LM}(4\pi/2L+1) \int d\hat{r}\, Y^*_{\ell,\Lambda-\lambda}(\hat{r}) Y_{LM}(\hat{r}) Y_{\ell'\Lambda-\lambda'}(\hat{r}) Y_{1m}(\hat{r}) \\ \times [r^{-L-1} \int_0^r d\vec{r}\, 1\sigma_g(\vec{r}') r'^{L} 1\sigma_g'(\vec{r}') Y_{LM}(\hat{r}') \\ + r^{L} \int_r^\infty d\vec{r}\, 1\sigma_g(\vec{r}') r'^{-L-1} 1\sigma_g'(\vec{r}') Y_{LM}(\hat{r})], \end{aligned} \tag{24}$$

the second integral is omitted because it is the contribution when the incident

electron lies inside the molecular electrons. On a similar ground the exchange interactions are ignored from consideration. Furthermore, we have omitted the coupling potentials between the ground and excited states due to polarized orbitals. This is consistent with the physical description of the incident electron being at a far distance where it "sees" the molecule in one or the other state.

The procedures of solving the CC integro-differential equations and of extracting cross sections from their asymptotic form are described in detail elsewhere,[8] and will not be repeated here.

IV. RESULTS AND DISCUSSION

The methods described in Secs. II and III are used to calculate the excitation ($X^1\Sigma_g^+ \rightarrow B^1\Sigma_u^+$) cross sections of H_2 molecule. The configurations of these states are:

$$X^1\Sigma_g^+ : \quad (1\sigma_g)^2$$
$$B^1\Sigma_u^+ : \quad (1\sigma_g)(1\sigma_u).$$

The unperturbed MO's are obtained by two separate SCF calculations and identical to those used in our previous work.[8] Polarized orbitals of σ_u, π_u^+, π_u^- symmetries are calculated from the parent $1\sigma_g$ of the ground state, and those of σ_g, π_g^+, π_g^- symmetries are calculated from $1\sigma_u$ orbital. Polarized orbitals from the parent $1\sigma_g$ of the $B^1\Sigma_u^+$ are also calculated. But, since they are much smaller in magnitude than those from the $1\sigma_u$ orbital, we have excluded them from further consideration. This is understandable because the $1\sigma_g$ (ε = -24.94 eV) orbital of the $B^1\Sigma_u^+$ state is much more tightly bound than $1\sigma_u$ (ε = -5.84 eV) and expected to be less susceptible to polarization. We obtained 4.78 a.u. for the isotropic component of the dipole polarizability of H_2, which is within 8% of the best calculated value 5.18 a.u. available.[10] This good agreement gives an independent check for the accuracy of our polarized orbitals.

The excitation cross sections are obtained at two representative energies of the incident electron and shown in Table I. For comparison we included in Table I cross sections obtained without polarized orbitals. The inclusion of polarized orbitals makes a significant ($\sim$35%) difference in the cross section at E = 25 eV, but much less change (9%) at E = 50 eV. This is consistent with the physical reasoning that polarization is a phenomenon of slow-electron scattering.

Unfortunately, the only available set of experimental cross sections[11] are in rather substantial disagreement from the close-coupling calculation with or without polarized orbitals included. One can only hope that independent measurements and calculations will clarify the situation.

From this study it is apparent that the target polarization is an important factor to be considered in the collision processes of molecules by slow electrons. However, theoretical means to achieve this goal needs further improvement.

REFERENCES

1. N. F. Lane, Rev. Mod. Phys. 52, 29 (1980).
2. R. K. Nesbet, Adv. At. Mol. Phys. 13, 315 (1977).
3. A. Temkin, Phys. Rev. 107, 1004 (1957); 116, 358 (1957); A. Temkin and J. C. Lamkin, ibid 121, 788 (1961).
4. D. R. Drachman and A. Temkin, in Case Studies in Atomic Collision Physics II, edited by E. W. McDaniel and M. R. C. McDowell (North-Holland, 1972), Chapt. 6.
5. P. G. Burke and T. G. Webb, J. Phys. B 3, L131 (1970).
6. R. J. W. Henry and N. F. Lane, Phys. Rev. 183, 221 (1969).
7. P. G. Burke and N. Chandra, J. Phys, B 5, 1696 (1972).
8. S. Chung and C. C. Lin, Phys. Rev. A 17, 1874 (1978).
9. Vo Ky Lan, J. Phys. B 5, 242 (1972).
10. W. Kolos and L. Wolniewicz, J. Chem. Phys. 46, 1926 (1967).
11. S. K. Srivastava and S. Jensen, J. Phys. B 10, 3341 (1977).

Table I. Direct excitation cross sections of the $B^1\Sigma_u^+$ state of H_2 in units of 10^{-17} cm^2.

Incident Energy (eV)	Close Coupling with Polarized Orbitals	Standard Close Coupling	Experiment[a]
25	5.8	4.3	2.0 ± 0.6[b]
50	5.1	4.7	2.8 ± 0.8

[a] Ref. 11

[b] Linear interpolation of measured values 1.9 ± 0.6 at 20 eV and 2.0 ± 0.6 at 30 eV.

PART IV

TRANSITION PROBABILITY OF THE $^1S_0 \rightarrow {}^1D_2$ EMISSION OF ATOMIC OXYGEN

I. INTRODUCTION

The dipole-forbidden transition $^1S_0 \rightarrow {}^1D_2$ (5577 Å) in OI is a prominent feature of auroral spectra, which has received a good deal of attention historically. The $^1S_0 \rightarrow {}^1D_2$ transition probability also plays an important role as a parameter in quantitative modeling of the earth's upper atmosphere, especially in establishing population densities of various atomic and molecular species and in determining mechanisms of production and quenching of them.[1]

The upper state $^1S_0$ also makes a magnetic dipole transition to the $^3P_1$ state (λ = 2972 Å) besides the 5577 Å emission. The transition probabilities of these lines as well as the lifetime of the $^1S_0$ state have been determined experimentally by numerous groups.[2-8] The experimental value of the Einstein A coefficient for the 5577 Å line is 1.06 ± 0.32 sec^{-1}, and the decay constant of the $^1S_0$ state [i.e., A(5577 Å) + A(2972 Å)] ranges from 1.11 to 1.43 sec^{-1}.[3] There have also been several theoretical calculations[9-13] with the resulting value of A between 1.183 and 2.2 sec^{-1}. The earlier calculations in which hydrogenic wave functions were employed are thought to have only limited accuracy.[9,10] More recently, Nicholaides et al.[13] obtained A(5577 Å) as 1.183 sec^{-1} based on wave functions computed by the method of "nonclosed-shell many-electron theory (NCMET)."

The effects of electron correlation, which were important distinguishing features of the work by Nicholaides et al., may be taken into account in a systematic way by the multiconfiguration Hartree-Fock (MCHF) method.[14] In view of the importance of the $^1S_0 \rightarrow {}^1D_2$ transition in atmospheric research, it is worthwhile to reexamine the theoretical transition probability from the MCHF approach.

II. METHOD OF CALCULATION AND RESULTS

The wave functions employed in this work have been computed by the MCHF method,[14] and are expressed in terms of linear combinations of single configuration functions ψ_i as

$$\Psi(^1S_0) = \Sigma_i\ a_i\psi_i(\vec{r}_1,\vec{r}_2,\ldots,\vec{r}_N|^1S_0), \tag{1}$$

and

$$\Psi(^1D_2) = \Sigma_i b_i\psi_i(\vec{r}_1,\vec{r}_2,\ldots,\vec{r}_N|^1D_2), \tag{2}$$

where a_i, b_i are configuration-mixing coefficients. The MCHF method is described in detail elsewhere.[14] Two sets of MCHF functions of the $^1S_0$ state are displayed in Table I showing the configurations and the corresponding coefficients as well as the computed total energy for each of the two sets. In the cases where more than one LS coupling term may be derived from an $(n\ell)^q$ configuration, a specific designation is written inside a square bracket. Similarly, we show two sets of the $^1D_2$ functions in Table II. In the present MCHF procedure, the orbitals and the configuration coefficients are optimized simultaneously so that the orbitals are common for all configurations within a state. Although no relationship need be imposed between sets of orbitals belonging to one state and of those belonging to the other state, the 1s, 2s, and 2p orbitals are held common to both the $^1S_0$ and $^1D_2$ states so that we may take advantage of the orthonormal property of the orbitals when evaluating the quadrupole matrix elements between the $^1S_0$ and $^1D_2$ states. Even with this restriction, we believe the wave functions are quite accurate as a sufficient number of configurations are included to account for effects such as electron correlations. For example, the computed $^1S_0$ - $^1D_2$ energy splitting is 0.086465 a.u. (5270 Å) from set A of Tables I and II, which is within 5.5% of

the observed value of 5577 Å. In studying the forbidden transitions, the fundamental quantity is the quadrupole line strength S defined[15] as

$$S(^1S_0,\ ^1D_2) = (2/3)e^2\ \Sigma_m|(4\pi/5)^{1/2}\int\Psi^*(\vec{r}_1,\vec{r}_2,..,\vec{r}_N|^1S_0)\times$$
$$\Sigma_s\ r_s^2\ Y_{2m}(\hat{r}_s)\ \Psi(\vec{r}_1,\vec{r}_2,..,\vec{r}_N|^1D_2)d\vec{r}_1d\vec{r}_2...d\vec{r}_N|^2, \tag{3}$$

where $Y_{\ell m}$ is the sperhical harmonic. The summation over m is merely formal since there is only one nonvanishing element, and the summation over s covers all eight atomic oxygen electrons. In the LS-coupling scheme, the quardupole transition probability is defined through the line strength as[15,16]

$$A(^1S_0 \rightarrow {}^1D_2) = 32\pi^6S(^1S_0,\ ^1D_2)/5h\lambda^5. \tag{4}$$

A related quantity is the quadrupole transition oscillator strength defined[17] as

$$f(^1S_0,{}^1D_2) = 4\pi^4mcS(^1S_0,{}^1D_2)/5he^2\lambda^3, \tag{5}$$

where m and c are the mass of electron and the speed of light respectively. With the wave functions in the MCHF form as in Eqs. (1) and (2), the line strength is now written as

$$S(^1S_0,{}^1D_2) = (2/3)e^2|\Sigma_{ij}I_{ij}|^2, \tag{6}$$

with

$$I_{ij} = a_ib_j(4\pi/5)^{1/2}\int\psi_i^*(\vec{r}_1,\vec{r}_2,\ldots,\vec{r}_N|^1S_0)\times$$
$$\Sigma_s\ r_s^2Y_{2m}(\hat{r}_s)\psi_j(\vec{r}_1,..,\vec{r}_N|^1D_2)d\vec{r}_1d\vec{r}_2...d\vec{r}_N, \tag{7}$$

where m is to take the particular value (from -2 to 2) that gives a nonvanishing integral. In Table III we display the contributions I_{ij} computed by Eq. (7)

along with the wave functions of set A in Tables I and II. We note from Table III that the primary configuration $1s^2 2s^2 2p^4$ alone gives 2.51 a_o^2 as compared with 2.42 a_o^2 when all contributions are summed (a_o being the Bohr radius). The corresponding values with the wave functions of set B are 2.55 a_o^2 and 2.48 a_o^2 respectively. The good agreement (3%) between the results from the larger (A) and smaller set (B) sets indicates that the wave functions of either set are reasonably accurate. By using our best value (2.42 a_o^2) and with λ = 5577 Å, we obtain 1.22 sec^{-1} for the transition probability and 5.69 x 10^{-9} for the oscillator strength.

From the off-diagonal hypervirial relation,[18,19]

$$\Sigma_s \, r_s^2 = (2/\Delta E) \, \Sigma_s \, \vec{r}_s \cdot \vec{\nabla}_s \, , \tag{8}$$

we obtain an equivalent expression of Eq. (7), i.e.,

$$I_{ij} = a_i b_j (4\pi/5)^{1/2} \, (2/\Delta E) \int \psi_i^* \, (r_1, r_2, .., r_N | {}^1S_0) \times$$

$$\Sigma_s \, Y_{2m}(\hat{r}_s) \, \vec{r}_s \cdot \vec{\nabla}_s \, \psi_j(\vec{r}_1, \vec{r}_2, \ldots, \vec{r}_N | {}^1D_2) \, d\vec{r}_1 d\vec{r}_2 \ldots d\vec{r}_N, \tag{9}$$

where ΔE is the energy difference in atomic units. When Eq. (9) is used to compute the integrals, the resulting strength is in the "velocity form" as opposed to the "length form" when Eq. (7) is used. We re-compute the oscillator strength with the velocity form and include in Table III the contributions from the various configurations. The velocity form gives an oscillator strength of 4.88 x 10^{-9} in reasonable agreement with the result of the length form. Furthermore, in the velocity form there is no contribution to the line strength from the dominant $1s^2 2s^2 2p^4$ configuration (Table III) so that this agreement is achieved through the inclusion of correlation. Thus the velocity form provides a critical test of the accuracy of the wave function. Both these observations render additional support to the accuracy of the wave functions used in this work.

III. DISCUSSION

The transition probability (1.22 sec^{-1}) of this work agrees very well with 1.28 sec^{-1} computed by Garstang[11,12] and 1.183 sec^{-1} by Nicholaides et al.[13] Garstang's value of 1.28 sec^{-1} is based on the single-configuration Hartree-Fock functions. This is in general accord with our finding that in the length form the primary configuration of $1s^2 2s^2 2p^4$ dominates over all others as shown in Table III. The close agreement with the result of Nicholaides et al. is particularly encouraging, since their method of computing the wave functions (NCMET) is quite different from the MCHF method adopted in this work. In Garstang's semiempirical study,[12] the effect due to the departure from the LS-coupling scheme is found to be very small; 1.25 sec^{-1} and 1.28 sec^{-1} respectively with and without such an effect. Therefore, it is unlikely that the theoretical value presented here will change significantly even with the inclusion of other effects such as spin-orbit coupling.

The experimental determination of the transition probability A(5577Å) is impeded by the difficulty of ascertaining the number density of the $^1S_0$ state and by the competing 2972Å ($^1S_0 \rightarrow {}^3P_1$) transition. However, McConkey and Kernahan[2] measure A(5577Å) to be 1.0 sec^{-1} from a discharge experiment. By using a similar technique, Kernahan and Pang[3] obtained a value of 1.06 ± 0.32 sec^{-1}. The greater certainty in the latter experiment is largely due to a more precise knowledge of the $^1S_0$ number density. Other experimental data relevant to this work are measurements of the radiative decay constant of the $^1S_0$ state, i.e., the sum of A(5577Å) and A(2972Å). Corney and Williams[8] obtained 1.31 ± 0.05 sec^{-1} for the decay constant Γ from

a laboratory experiment. From the analysis of aurora observation, Omholt[4], and Evans and Jones[5] deduced Γ as 1.43 and 1.49 sec^{-1} respectively. In addition the A(5577Å)/A(2972Å) ratio has been reported as 18.6 by McConkey et al.[7], 22 by Le Blanc et al.[6], and 23.7 by Kernahan and Pang.[2] From the experimental data of the decay constant and of the A(5577Å)/A(2972Å) ratio, we estimate the value of A(5577Å) to be in the range of 1.24 sec^{-1} to 1.37 sec^{-1}.

The direct measurement 1.06 ± 0.32 sec^{-1} by Kernahan and Pang[2] is somewhat smaller than our theoretical value 1.22 sec^{-1}, though the latter is well within the stated uncertainty of the experimental data. On the other hand the "deduced values" (1.24 - 1.37 sec^{-1}) are somewhat greater than the theoretical value. Considering the experimental difficulties and uncertainties, it is encouraging to see this essential agreement between theory and experiment. The good agreement of our calculation with the previous theoretical works[11-13], where realistic wave functions were used, also gives a greater confidence in the A(5577Å) value presented here.

The research presented in Part IV was done in collaboration with Professor Charlotte F. Fischer of the Vanderbilt University. The part of the work contributed by Professor Fischer was not supported by the Air Force Geophysics Laboratory. A paper entitled "Transition Probability of the $^1S_0 \rightarrow {}^1D_2$ Emission of Atomic Oxygen" has been published jointly with Professor Fischer in the Journal of Chemical Physics, Volume 76, pp. 498-501(1982).

REFERENCES

1. R. R. O'Neil, E. T. P. Lee, and E. R. Huppi, J. Geophys. Res. 84, 823 (1979).
2. J. W. McConkey and J. A. Kernahan, Planet. Space. Sci. 17, 1297 (1969).
3. J. A. Kernahan and P. H-L. Pang, Can. J. Phys. 53, 455 (1975).
4. A. Omholt, in The Airglow and the Aurorae, edited by E. B. Armstrong and A. Dalgarno (Pergamon Press, New York, 1956), p. 178.
5. W. F. J. Evans and A. Vallance Jones, Can. J. Phys. 43, 697 (1965).
6. F. S. Le Blanc, O. Oldenberg, and N. P. Carleton, J. Chem. Phys. 45, 2200 (1966).
7. J. W. McConkey, D. J. Burns, K. A. Moran, and K. G. Emeleus, Phys. Letters 22, 416 (1966).
8. A. Corney and O. M. Williams, J. Phys. B 5, 686 (1972).
9. E. U. Condon, Astrophys. J. 79, 217 (1934).
10. S. Pasternack, Astrophys. J. 92, 129 (1940).
11. R. H. Garstang, Mon. Not. Roy. Astron. Soc. 111, 115 (1951).
12. R. H. Garstang, in The Airglow and the Arorae, edited by E. B. Armstrong and A. Dalgarno (Pergamon Press, New York, 1956), p. 324.
13. C. Nicholaides, O. Sinanoğlu and P. Westhaus, Phys. Rev. A 4, 1400 (1971).
14. C. Froese Fischer, Comput. Phys. Commun. 4, 107 (1972); 7, 236 (1974).
15. R. H. Garstang, Proc. Camb. Phil. Soc. 53, 214 (1957); M. J. Seaton, Proc. Roy. Soc. A 231, 37 (1955).
16. E. G. Condon and G. A. Shortley, The Theory of Atomic Spectra, (Cambridge University Press, 1963), Ch. IV.
17. I. I. Sobel'man, Introduction to the Theory of Atomic Spectra, (Pergamon Press, Oxford, 1972), Sec. 32.
18. M. Godefroid, Comput. Phys. Commun. 15, 275 (1978).
19. J. C. Y. Chen, J. Chem. Phys. 40, 615 (1964).

Table I. Multiconfiguration Wave Function of Oxygen ^1S State.

	Configuration [a]	Coefficients	
		Set A [b]	Set B [c]
1.	$(2s)^2(2p)^4$	0.970 206	0.978 474
2.	$(2p)^6$	0.189 263	0.201 885
3.	$(2p)^4[^1D](3p_1)^2$	0.005 880	0.010 334
4.	$(2s)^2(2p)^3[^2P](3p_2)$	0.018 115	-0.011 121
5.	$(2p)^5(3p_3)$	-0.028 477	0.030 984
6.	$(2s)(2p)^4[^1D](3d_1)$	0.030 612	0.025 077
7.	$(2s)(2p)^4[^1D](3s_1)$	0.000 625	0.003 363
8.	$(2s)^2(2p)^2[^1S](3p_4)^2[^1S]$	-0.072 190	
9.	$(2s)^2(2p)^2[^3P](3p_4)^2[^3P]$	0.053 232	
10.	$(2s)^2(2p)^2[^1D](3p_4)^2[^1D]$	0.059 830	
11.	$(2s)^2(2p)^2[^1S](3s_2)^2$	0.022 216	
12.	$(2p)^4[^1S](3s_2)^2$	-0.019 487	
13.	$(2s)^2(2p)^2[^1S](3d_2)^2[^1S]$	0.067 818	
14.	$(2s)^2(2p)^2[^3P](3d_2)^2[^3P]$	-0.044 863	
15.	$(2s)^2(2p)^2[^1D](3d_2)^2[^1D]$	-0.040 721	
	Energy	-74.759 539 a.u.	-74.670 000 a.u.

a) Subscripts indicate different orbitals of the same type.

b) 1s, 2s, and 2p orbitals from fully variational MCHF calculation for first three configurations; all other orbitals variational.

c) 1s, 2s, 2p and $3p_1$ orbitals from fully variational MCHF calculation for first three configurations; all other orbitals variational.

Table II. Multiconfiguration Wave Function of Oxygen ^1D State.

	Configuration [a]	Coefficients	
		Set A [b]	Set B [c]
1.	$(2s)^2(2p)^4$	0.984 825	0.993 420
2.	$(2p)^4[^1D](3p_1)^2$	0.016 950	0.016 257
3.	$(2s)^2(2p)^3[^2P](3p_2)$	-0.020 586	-0.028 079
4.	$(2s)^2(2p)^3[^2D](3p_2)$	-0.000 783	-0.006 358
5.	$(2p)^5(3p_3)$	-0.029 366	-0.029 958
6.	$(2s)(2p)^4[^1S](3d_1)$	0.000 962	-0.000 508
7.	$(2s)(2p)^4[^3P](3d_1)$	-0.103 608	-0.105 378
8.	$(2s)(2p)^4[^1D](3d_1)$	0.002 907	-0.000 497
9.	$(2s)(2p)^4[^1D](3s_1)$	-0.005 460	-0.004 695
10.	$(2s)^2(2p)^2[^1S](3p)^2[^1D]$	0.026 074	
11.	$(2s)^2(2p)^2[^3P](3p_4)^2[^3P]$	0.054 850	
12.	$(2s)^2(2p)^2[^1D](3p_4)^2[^3P]$	0.035 520	
13.	$(2s)^2(2p)^2[^1D](3p_4)^2[^1D]$	0.070 313	
14.	$(2s)^2(2p)^2[^1D](3s_2)^2$	-0.010 932	
15.	$(2p)^4[^1D](3s_2)^2$	-0.023 824	
16.	$(2s)^2(2p)^2[^1S](3d_2)^2[^1D]$	-0.015 317	
17.	$(2s)^2(2p)^2[^3P](3d_2)^2[^3P]$	-0.045 117	
18.	$(2s)^2(2p)^2[^1D](3d_2)^2[^1S]$	-0.034 052	
19.	$(2s)^2(2p)^2[^1D](3d_2)^2[^1D]$	0.043 443	
20.	$(2s)^2(2p)^3[^2P](4f)$	0.024 741	
21.	$(2s)^2(2p)^3[^2D](4f)$	0.035 528	
	Energy	-74.846 004 a.u.	-74.770 167 a.u.

a) Subscripts indicate different orbitals of the same type.

b) 1s, 2s, 2p orbitals fixed as in Set A of Table 1; all other orbitals variational.

c) 1s, 2s, 2p and $3p_1$ orbitals as in Set B of Table 1; all other orbitals variational.

Table III. Contributions to quadrupole matrix element I_{ij}.

Configurations		I_{ij}	
$^1S_0$	$^1D_2$	by Eq. (7)	by Eq. (9)
1	1	2.511 346	0.0
1	3	-0.062 992	-0.528 617
1	6	-0.002 412	-0.054 722
1	20	-0.092 596	-2.381 701
2	5	0.020 423	0.163 222
4	1	0.026 269	-0.162 122
4	3	-0.002 158	0.004 720
4	20	-0.001 001	0.007 322
5	5	-0.002 600	0.000 022
6	1	-0.029 648	0.741 202
8	3	0.002 121	-0.021 689
8	10	0.009 408	-0.001 819
8	13	0.006 737	0.0
9	3	-0.001 173	0.011 995
9	11	0.011 132	-0.001 410
10	10	-0.001 833	0.0
10	12	-0.004 750	0.000 918
10	13	0.018 978	-0.002 404
12	15	0.001 220	0.0
13	16	0.006 444	-0.001 246
13	18	0.006 069	0.0
14	17	0.010 087	-0.001 435
15	18	-0.003 847	0.000 744
Others		-0.000 282	-0.018 289
TOTAL		2.424 942	-2.245 309

PUBLICATIONS

The following papers have been published under the sponsorship of this contract.

1. Thomas K. Holley, Sunggi Chung, Chun C. Lin and Edward T. P. Lee, Phys. Rev. A 24, 2946 (1981).
2. Sunggi Chung, Chun C. Lin, Charlotte F. Fischer, and Edward T. P. Lee, J. Chem. Phys. 76, 498 (1982).
3. Thomas K. Holley, Sunggi Chung, Chun C. Lin, and Edward T. P. Lee, (submitted for publication in Phys. Rev. A).

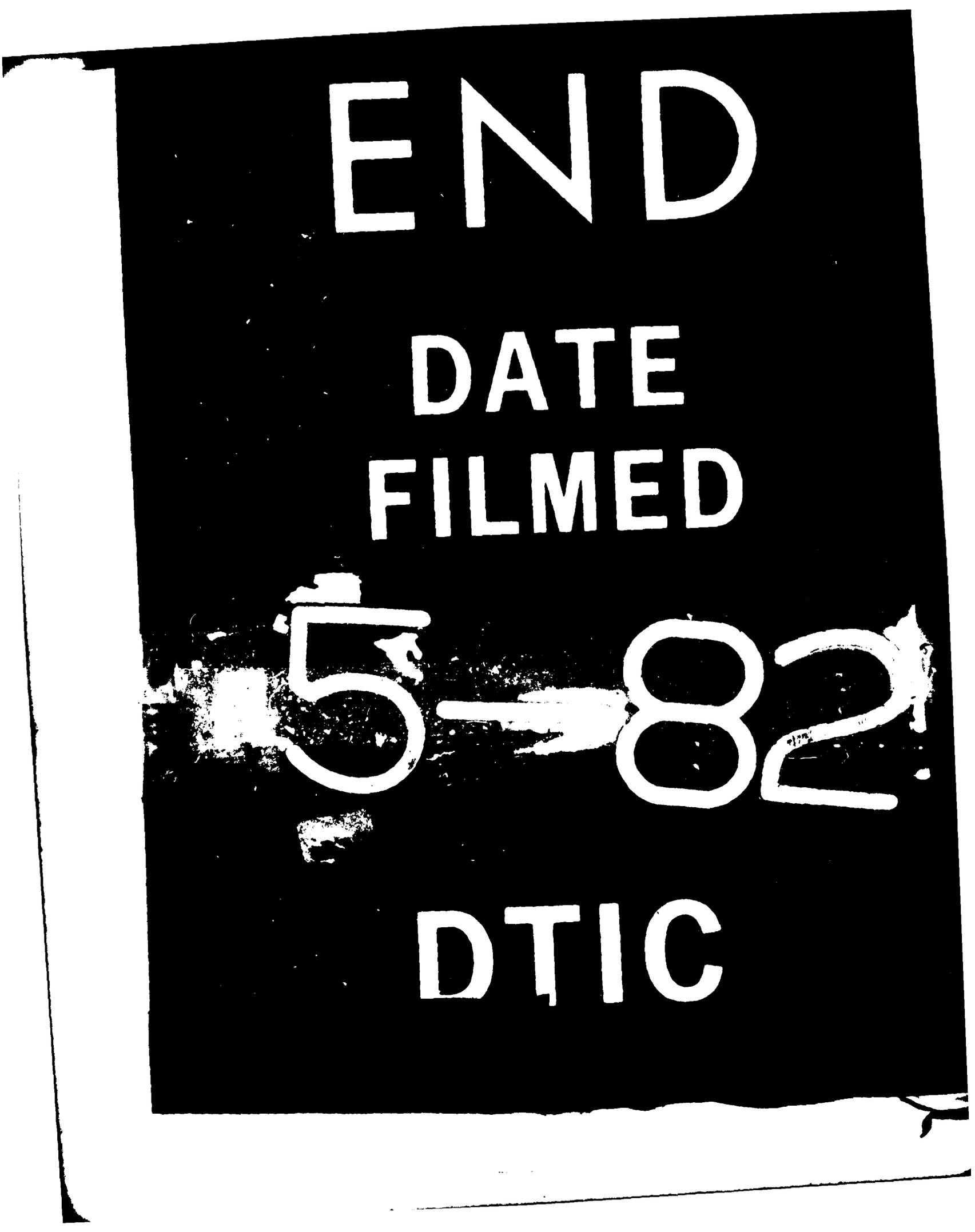
END
DATE
FILMED
5-82
DTIC